



HAL
open science

Robust leader-follower formation control of autonomous vehicles with unknown leader velocities

Anes Lazri, Esteban Restrepo, Antonio Loria

► **To cite this version:**

Anes Lazri, Esteban Restrepo, Antonio Loria. Robust leader-follower formation control of autonomous vehicles with unknown leader velocities. 2023 European Control Conference (ECC 2023), Jun 2023, Bucharest, Romania. pp.1–6, 10.23919/ECC57647.2023.10178165 . hal-03869953v2

HAL Id: hal-03869953

<https://hal.science/hal-03869953v2>

Submitted on 31 Oct 2023

HAL is a multi-disciplinary open access archive for the deposit and dissemination of scientific research documents, whether they are published or not. The documents may come from teaching and research institutions in France or abroad, or from public or private research centers.

L'archive ouverte pluridisciplinaire **HAL**, est destinée au dépôt et à la diffusion de documents scientifiques de niveau recherche, publiés ou non, émanant des établissements d'enseignement et de recherche français ou étrangers, des laboratoires publics ou privés.

Robust leader-follower formation control of autonomous vehicles with unknown leader velocities

Anes Lazri Esteban Restrepo Antonio Loría

Abstract—We address the problem of formation-tracking control of velocity-controlled unicycles in a leader-follower configuration, both with known and unknown leader velocities. The controller design is based on relative measurements: distances and line-of-sight angles. This type of measurements are provided by onboard sensors rather than global positioning systems. We assume that a virtual leader generates a desired reference trajectory for the whole swarm, that is once continuously differentiable, bounded and with bounded derivative. We propose two controllers, one for which it is assumed that the leader velocities are known and one in which they are unknown.

Index Terms—Nonholonomic multi-agent systems, formation control, output feedback

I. INTRODUCTION

The formation control problem of nonholonomic vehicles consists in controlling a group of robots to perform a desired formation around a given point or follow a trajectory [1], [2]. Such problem has been addressed in the literature via time-varying controls [3] [4], or time-invariant discontinuous controls [5].

The time-varying control laws often rely on persistency-of-excitation and are attractive since they often ensure uniform convergence properties, thereby implying robustness [6].

In [7], the leader-follower time-varying formation control problem is considered using bearing measurements; the proposed control law consists of two parts, a proportional part that is used to stabilize the agents to the target formation and an integral part that is used to eliminate static errors when the leader's velocity is time-varying. An inconvenience of persistency-of-excitation-based controllers, however, is that they are difficult to tune since they may present oscillatory transients [4]. The bearing-based formation control is also used in [8] in the case of discontinuous control. This problem can also be encountered in the case of discontinuous control; in [5] an inter-agent damping injection technique based on passivity proposed to eliminate the relative motion oscillatory and steady formation error.

An alternative approach, which allows to use time-invariant controllers, relies on a polar-coordinates-based model. In [9] a controller is proposed for unicycles modeled in polar coordinates, which leads to smooth closed control

laws and is suitable for steering and path following. It is also important to note that many polar-coordinate models are equivalent. In [10] decentralized second-order sliding-mode control laws are proposed to solve the formation-control problem in a leader-follower scheme. On the other hand, in [11], a polar-coordinates model with two variables is used, and a control law that ensures the formation tracking using Barrier Lyapunov functions is proposed. Another equivalent polar-coordinates model is used in [12], which allows solving the formation problem with a time-invariant controller that is continuous along trajectories and does not require global position measurements.

Now, in many works, it is assumed that the follower robots have access to their leaders' velocities [11] [12]. However, this may appear conservative in some cases. Hence one can instead rely on certainty-equivalence controllers and velocity estimation. In [13] a sliding-mode-based estimation and a formation tracking controller are proposed for the error dynamics based on the Cartesian model of the system. See also [14], where an adaptive control technique is proposed for estimating the leader's velocities to solve a leader-follower formation problem. A way to solve the velocity estimation problem for the polar-coordinates model used in [12] was proposed in [15]. The latter addresses the formation control of nonholonomic mobile robots with visual servoing. The proposed controller requires pose estimation, but not velocity measurements.

In this paper we propose a polar-coordinates-based, time-invariant, formation-tracking controller and a linear and angular velocity observer which relies only on relative measurements. Compared to the literature, we consider the polar-coordinates model used in [16], but we emphasize that [16] is devoted to the formation-consensus problem. We assume the robots advance in a leader-follower configuration, forming a multi-agent system with an underlying directed spanning-tree topology. We address both cases in which the leaders' velocities are known and unknown to the follower.

The remainder of this paper is organized as follows. In Section II, we present the problem formulation. Our results are presented in Section III. Section IV contains an illustrative example, and concluding remarks are given in Section V.

A. Lazri is with the Laboratoire des signaux et systèmes (L2S), Univ Paris-Saclay; L2S-CentraleSupélec, 3, Rue Joliot-Curie, Gif sur Yvette, France. E-mail: Anes Lazri anes.lazri@centralesupelec.fr. A. Loría is with L2S, CNRS, France. E-mail: antonio.loria@cnsr.fr. E. Restrepo is with CNRS-INRISA, Inria Rennes, France. E-mail: esteban.restrepo@inria.fr.

This work was supported by CEFIPRA under the grant number 6001-A. The work of A. Loría was also supported by the French ANR via project HANDY, contract number ANR-18-CE40-0010.

II. MODEL AND PROBLEM FORMULATION

Autonomous nonholonomic vehicles may be modelled using the kinematics equations

$$\dot{x}_j = v_j \cos(\theta_j) \quad (1a)$$

$$\dot{y}_j = v_j \sin(\theta_j) \quad (1b)$$

$$\dot{\theta}_j = \omega_j, \quad j \in \{1, 2, \dots, N\}, \quad (1c)$$

where $p_j = [x_j \ y_j]^\top \in \mathbb{R}^2$ denotes the position in Cartesian coordinates of the vehicle's center of mass on the plane and $\theta_j \in [-\pi, \pi]$ denotes its orientation with respect to the axis of the abscissae. If the vehicle is velocity-controlled (which is often the case), the forward and angular velocities, v_j and ω_j , constitute the control inputs. When absolute position and orientation measurements with respect to a fixed frame, (p_j, θ_j) , are available, the model above is most appropriate. Then, the leader-follower tracking control problem consists in making a robot, modelled by the kinematics equations above, follow a leader robot.

In many applications, however, absolute measurements are unavailable. Instead, the robot is equipped with relative-measurement sensors, which deliver the distance separating the leader from the follower, they can also deliver the relative orientation with respect to the line of sight. We use ρ_k to denote such distance, β_k to denote the angle of the leader robot relative to the follower's line of sight and α_k to denote the orientation of the follower relative to the same line. See Figure 1.

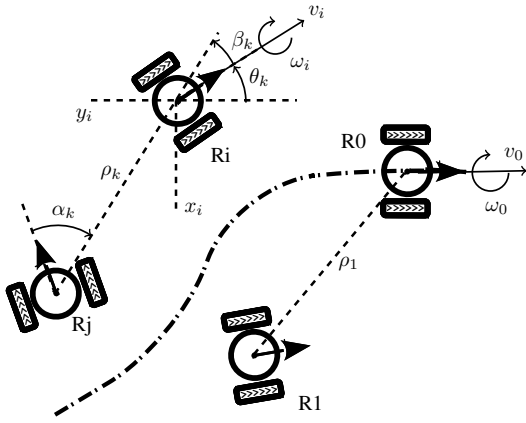


Fig. 1. Leader-follower formation with relative measurements (in polar coordinates)

It is assumed that for a swarm of robots each vehicle follows one and only one leader. For instance, in Figure 1 the vehicle 'Rj' follows the vehicle 'Ri', while 'R1' — called swarm leader— follows the virtual reference robot 'R0', which moves freely with forward and angular velocities v_0 and ω_0 respectively.

In general, for a swarm of N robots, the leader-follower interaction among all the robots may be modelled by a spanning-tree graph with $N - 1$ edges —see Figure 2. The multi-agent system, modelled as a spanning tree consists in

a collection of open chains of leader-follower robots which, in turn, consists in a series of pairs of robots (Rj,Ri).

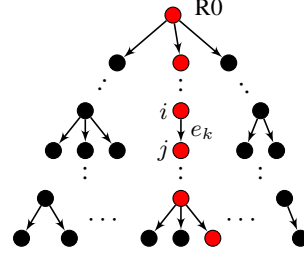


Fig. 2. Graph interconnections in a Leader-follower formation configuration with relative measurements

In function of the relative Cartesian coordinates and the absolute orientations of each robot of the pair $k = (i, j)$, we have for each $k \in \{0, 1, \dots, N - 1\}$.

$$\rho_k = |p_i - p_j|, \quad (2a)$$

$$\beta_k = \arctan\left(\frac{y_i - y_j}{x_i - x_j}\right) - \theta_i \quad \forall \rho_k > 0 \quad (2b)$$

$$\alpha_k = \arctan\left(\frac{y_i - y_j}{x_i - x_j}\right) - \theta_j \quad \forall \rho_k > 0. \quad (2c)$$

Differentiating on both sides of (2)

$$\dot{\rho}_k = v_i \cos(\beta_k) - v_j \cos(\alpha_k) \quad (3a)$$

$$\dot{\beta}_k = \frac{1}{\rho_k} [-v_i \sin(\beta_k) + v_j \sin(\alpha_k)] - \omega_i \quad (3b)$$

$$\dot{\alpha}_k = \frac{1}{\rho_k} [-v_i \sin(\beta_k) + v_j \sin(\alpha_k)] - \omega_j, \quad (3c)$$

In the latter, v_i and ω_i are the velocities of the leader for a leader-follower pair (i, j) , which are considered as external reference signals, and v_j and ω_j are the control inputs. Equations (3) model the dynamics of the relative distance and orientations of any pair of robots.

Note that the relative angles are defined only for all $\rho_k > 0$, which is meaningful because $\rho_k = 0$ means that two robots occupy the same physical space, which is impossible. Therefore, for a swarm of N robots we define the leader-follower formation tracking problem as that of making for each k (for as many pairs of leader-follower robots existing in the swarm),

$$\lim_{t \rightarrow +\infty} \rho_k(t) = \rho_k^* \quad (4a)$$

$$\lim_{t \rightarrow +\infty} \beta_k(t) = \beta_k^*, \quad (4b)$$

for any given constant relative distance ρ_k^* and any desired constant relative orientation β_k^* .

From a control viewpoint, the leader-follower formation tracking control problem may be cast as that of stabilizing (ρ_k^*, β_k^*) for the dynamical system (3).

III. MAIN RESULTS

The control design consists in finding control laws v_j and ω_j for the system (3) to stabilize (ρ_k^*, β_k^*) for all $k \leq N$ —we consider that there are N physical vehicles and one virtual leader R0, so the tree contains N edges.

The controller approach, on one hand, is based on Backstepping and barrier functions to guarantee collision avoidance. On the other hand, we design a leader-velocity observer. Then, we implement a certainty-equivalence output-feedback controller. For clarity of exposition, in section II-A we present first a state-feedback controller and in section II-B, we present our controller without leader velocity estimation.

A. Control design with known leader velocities

Assume that v_i and ω_i are known. Then, the backstepping controller is designed as follows. For the sake of argument, consider Eq. (3a) and let $u_\rho(v_j, \alpha_k) := v_j \cos(\alpha_k)$ be a virtual control input. Clearly, if

$$u_\rho(v_j, \alpha_k) = v_i \cos(\beta_k) + \nu_{\rho_k}, \quad \tilde{\rho}_k := \rho_k - \rho_k^* \quad (5)$$

with $\nu_{\rho_k} := -\lambda_1 \tilde{\rho}_k$, we obtain the closed-loop equation

$$\dot{\tilde{\rho}}_k = -\lambda_1 \tilde{\rho}_k, \quad (6)$$

for which the origin $\{\tilde{\rho}_k = 0\}$ is exponentially stable, so (4a) holds. However, even if such control action may be implemented, it carries two disadvantages. First, ρ_k may approach or be equal to zero, which not only means that the robots Ri and Rj collide, but it also renders the dynamical system (3) ill-posed. Therefore, we redefine ν_{ρ_k} as a gradient control law, derived from a *Barrier* function $\tilde{\rho}_k \mapsto B_k(\tilde{\rho}_k)$, that is, we set

$$\nu_{\rho_k} := -\lambda_1 \nabla B_k(\tilde{\rho}_k). \quad (7)$$

The Barrier function B_k is to be designed to take values in $\mathcal{D}_k := (-\rho_k^*, \rho_k^*)$ to produce image points in the right orthant of the Euclidean space, $\mathbb{R}_{\geq 0}$. By construction, it is required that $B_k(\tilde{\rho}_k) \rightarrow \infty$ as $\tilde{\rho}_k \rightarrow \partial \mathcal{D}_k$. We see that

$$B_k(\tilde{\rho}_k) := \frac{1}{2} \ln \left[\frac{\rho_k^{*2}}{\rho_k^{*2} - \tilde{\rho}_k^2} \right] + \tilde{\rho}_k^2 \quad (8)$$

satisfies such requirements. Moreover, $B_k(\rho_k - \rho_k^*) \rightarrow \infty$ as $\rho_k \rightarrow 0$ or $\rho_k \rightarrow 2\rho_k^*$. Under these conditions, Eq. (6) becomes

$$\dot{\tilde{\rho}}_k = -\lambda_1 \nabla B_k(\tilde{\rho}_k) \quad (9)$$

and a direct computation using B_k as a (Barrier) Lyapunov function for the latter, establishes that the origin $\{\tilde{\rho}_k = 0\}$ is asymptotically stable for all initial conditions in the domain of definition \mathcal{D}_k . Moreover, because $B_k(\tilde{\rho}_k) \rightarrow \infty$ as $\tilde{\rho}_k \rightarrow \partial \mathcal{D}_k$ it follows that $\rho_k(t) \in (0, 2\rho_k^*)$ for all $t \geq 0$. Since, by definition, $u_\rho(v_j, \alpha_k) := v_j \cos(\alpha_k)$, it is left to find α_k^* and v_j such that

$$v_j \cos(\alpha_k^*) = v_i \cos(\beta_k) + \nu_{\rho_k} \quad (10)$$

for any given ν_{ρ_k} . The obvious choice for v_j is

$$v_j := \frac{v_i \cos(\beta_k) + \nu_{\rho_k}}{\cos(\alpha_k^*)}, \quad (11)$$

which is well-defined for all $\alpha_k^* \in (-\pi/2, \pi/2)$. We pose

$$\alpha_k^* := \arctan(\psi_k). \quad (12)$$

We recall that

$$\cos(\arctan(\psi_k)) := \frac{1}{\sqrt{1 + \psi_k^2}}, \quad (13)$$

so (11) is equivalent to

$$v_j := [1 + \psi_k^2]^{1/2} [v_i \cos(\beta_k) + \nu_{\rho_k}], \quad (14)$$

which is well-defined for any finite ψ_k .

It is left to design ψ_k such that $\alpha_k = \alpha_k^*$, with α_k^* as in (12) stabilizes β_k^* for (3b). In other words, we consider α_k as a virtual control input in the latter equation. Hence, setting $\alpha_k = \alpha_k^*$ in (3b), and using

$$\sin(\arctan(\psi_k)) = \frac{\psi_k}{\sqrt{1 + \psi_k^2}} \quad (15)$$

and (14), we obtain

$$\dot{\beta}_k = \frac{1}{\rho_k} \left[-v_i \sin(\beta_k) + \psi_k [v_i \cos(\beta_k) + \nu_{\rho_k}] \right] - \omega_i, \quad (16)$$

so we define

$$\psi_k(t, e_k) = \frac{v_i \sin(\beta_k) - [\lambda_2 \tilde{\beta}_k - \omega_i] \rho_k}{v_i \cos(\beta_k) + \lambda_1 \nabla B_k(\tilde{\rho}_k)}, \quad (17)$$

where $\lambda_2 > 0$ and $e_k := [\tilde{\rho}_k \ \tilde{\beta}_k \ \tilde{\alpha}_k]^\top$ and, to avoid a cumbersome notation, we replaced $(\tilde{\rho}_k + \rho_k^*)$ with ρ_k , $(\tilde{\beta}_k + \beta_k^*)$ with β_k and the leader velocity v_i is considered as a function of time. Strictly speaking, however, it is a function of the leader's states, so $v_i(t)$ is considered as a functional of the leader's trajectories.

Finally, we use the second control input, ω_j to steer $\alpha_k \rightarrow \alpha_k^*$. Therefore, after (3c), we define

$$\omega_j := \frac{1}{\rho_k} \left[-v_i \sin(\beta_k) + v_j \sin(\alpha_k^*) \right] - \dot{\alpha}_k^* + \lambda_3 \tilde{\alpha}_k, \quad (18)$$

with $\tilde{\alpha}_k = \alpha_k - \alpha_k^*$ so that in closed loop we obtain

$$\dot{\tilde{\alpha}}_k = -\lambda_3 \tilde{\alpha}_k, \quad (19)$$

which is exponentially stable.

Thus, the previous reasoning leads to a nonlinear controller defined by

$$v_j := [1 + \psi_k^2]^{1/2} [v_i \cos(\beta_k) - \lambda_1 \nabla B_k(\tilde{\rho}_k)] \quad (20a)$$

$$\omega_j := \frac{1}{\rho_k} \left[-v_i \sin(\beta_k) + v_j \sin(\alpha_k) \right] - \dot{\alpha}_k^* + \lambda_3 \tilde{\alpha}_k + \nu_{\omega_k}, \quad (20b)$$

where ψ_k is defined in (17), B_k is defined in (8) and ν_{ω_k} is a redesign control input to be defined. As before, we made the choice of avoiding a cumbersome notation, but it is worth remarking that the terms on the respective right-hand sides of (20a) and (20b) are functions of time, through the leader's velocities $v_i(t)$ and $\omega_i(t)$ and of the errors e_k .

Remark 1: For the purpose of implementation without the exact derivative $\dot{\alpha}_k^*$, one can use command filtered backstepping [17], [18] or a simple approximate differentiator—cf. [19], [20],

$$H(s) = \frac{bs}{s+a}. \quad (21)$$

With α_k^* as input, in state space form, we define

$$\dot{\alpha}_{kf} = -a\alpha_{kf} + b\alpha_k^*, \quad (22)$$

and we use $\dot{\alpha}_{kf}$ in place of $\dot{\alpha}_k^*$.

We have the following.

Proposition 1: Consider $N - 1$ pairs of autonomous vehicles in a leader-follower configuration, each modelled as in (3) and forming a directed spanning tree —cf. Figure 2. For each vehicle, labeled j with $j \in \mathbb{N}_{\leq N}$, consider the controller defined by Eqs. (20), (8), (17) and

$$\nu_{\omega_k} := \frac{v_j}{\tilde{\alpha}_k} \left[\frac{\tilde{\beta}_k}{\rho_k} [\sin(\alpha_k) - \sin(\alpha_k^*)] - \nabla B_k(\tilde{\rho}_k) [\cos(\alpha_k) - \cos(\alpha_k^*)] \right], \quad (23)$$

for each $k \leq N - 1$. Then, the limits in (4) hold and the vehicles achieve formation tracking control of the leader robot R0. Moreover, $\rho_k(t) \in (0, 2\rho_k^*)$ for all $t > 0$, provided that $\rho_k(0) \in (0, 2\rho_k^*)$.

Proof: We start by writing the closed-loop equations in a suitable form, in terms of the errors $(\tilde{\rho}_k, \tilde{\beta}_k, \tilde{\alpha}_k)$. To that end, consider Eqs. (3a) and (3b),

$$\begin{aligned} \dot{\tilde{\rho}}_k &= v_i \cos \beta_k - v_j \cos \alpha_k^* + v_j \cos \alpha_k^* - v_j \cos \alpha_k \quad (24) \\ \dot{\tilde{\beta}}_k &= \frac{1}{\rho_k} [-v_i \sin(\beta_k) + v_j \sin(\alpha_k) \\ &\quad - v_j \sin(\alpha_k^*) + v_j \sin(\alpha_k^*)] - \omega_i. \quad (25) \end{aligned}$$

Then, we use (12), (13), (14), and (17) in the second term in (24) to obtain

$$\dot{\tilde{\rho}}_k = -\lambda_1 \nabla B_k(\tilde{\rho}_k) - v_j [\cos(\tilde{\alpha}_k + \alpha_k^*) - \cos(\alpha_k^*)]. \quad (26)$$

The arguments of α_k^* , i.e., $\tilde{\rho}_k$ and $\tilde{\beta}_k$, are omitted to avoid a cumbersome notation.

On the other hand, proceeding as shown above to obtain (19), we see that in view of (12), (14) and (15),

$$-v_i \sin(\beta_k) + v_j \sin(\alpha_k^*) = -\lambda_2 \tilde{\beta}_k.$$

It follows that the error equation for $\tilde{\beta}_k$ becomes

$$\dot{\tilde{\beta}}_k = -\lambda_2 \tilde{\beta}_k + \frac{v_j}{\rho_k} [\sin(\tilde{\alpha}_k + \alpha_k^*) - \sin(\alpha_k^*)]. \quad (27)$$

Finally, using (20b) in (3c) we obtain, by direct computation,

$$\dot{\tilde{\alpha}}_k = -\lambda_3 \tilde{\alpha}_k - \nu_{\omega_k}. \quad (28)$$

Next, consider the Barrier Lyapunov function $V_{1k} : \mathcal{D}_k \times \mathbb{R}^2 \rightarrow \mathbb{R}_{\geq 0}$ defined as

$$V_{1k}(e_k) := B_k(\tilde{\rho}_k) + \frac{1}{2} [\tilde{\beta}_k^2 + \tilde{\alpha}_k^2], \quad (29)$$

which is positive definite and radially unbounded in its domain of definition. The total derivative of V_{1k} along the trajectories of the closed-loop dynamics (26), (27), and (28), yields

$$\begin{aligned} \dot{V}_{1k}(e_k) &= -\lambda_2 \tilde{\beta}_k^2 + \tilde{\beta}_k \frac{v_j}{\rho_k} [\sin(\tilde{\alpha}_k + \alpha_k^*) - \sin(\alpha_k^*)] \\ &\quad - \lambda_1 \nabla B_k(\tilde{\rho}_k)^2 - \nabla B_k(\tilde{\rho}_k) v_j [\cos(\tilde{\alpha}_k + \alpha_k^*) - \cos(\alpha_k^*)] \\ &\quad - \lambda_3 \tilde{\alpha}_k^2 - \tilde{\alpha}_k \nu_{\omega_k}. \quad (30) \end{aligned}$$

Using (23) above we obtain that

$$\dot{V}_{1k}(e_k) = -\lambda_1 \nabla B_k(\tilde{\rho}_k)^2 - \lambda_2 \tilde{\beta}_k^2 - \lambda_3 \tilde{\alpha}_k^2. \quad (31)$$

That is, \dot{V}_{1k} is negative definite on its domain of definition, so we conclude that the origin $\{(\tilde{\rho}_k, \tilde{\beta}_k, \tilde{\alpha}_k) = 0\}$, for the closed-loop system, is asymptotically stable. In particular, the limits in (4) hold for any $k \leq N - 1$. Also, since by design $B_k(\tilde{\rho}_k(t)) \rightarrow \infty$ as $|\tilde{\rho}_k(t)| \rightarrow \rho_k^*$ it follows that $|\tilde{\rho}_k(t)| \leq \rho_k^*$ for all $t > 0$ and, consequently, $\rho_k(t) \in (0, 2\rho_k^*)$ for all $t > 0$ as required. ■

B. Control design with unknown leader velocities

To relax the assumption that the leader velocities are known to the followers, we redesign the controller from the previous section using the certainty-equivalence principle and a simple passivity-based adaptation law. Let \hat{v}_i and $\hat{\omega}_i$ denote estimates of the forward and angular leader velocities respectively and let $\bar{v}_i := \hat{v}_i - v_i$ and $\bar{\omega}_i := \hat{\omega}_i - \omega_i$ denote the estimation errors.

Inspired by [14], we introduce the following observer:

$$\dot{\hat{\omega}}_i := -\lambda_5 \hat{\omega}_i - \frac{1}{K_2} \tilde{\beta}_k \quad (32a)$$

$$\begin{aligned} \dot{\hat{v}}_i &:= -\lambda_4 \hat{v}_i + \frac{1}{K_1} \nabla B_k(\tilde{\rho}_k) \cos(\tilde{\beta}_k + \beta_k^*) \\ &\quad - \frac{\sin \beta_k}{\rho_k} (\tilde{\beta}_k + \tilde{\alpha}_k), \quad (32b) \end{aligned}$$

that we use with the certainty-equivalence control:

$$v_j := [1 + \hat{\psi}_k^2]^{1/2} [\hat{v}_i \cos(\beta_k) + \lambda_1 \nabla B_k(\tilde{\rho}_k)] \quad (33a)$$

$$\begin{aligned} \omega_j &:= \frac{1}{\rho_k} [-\hat{v}_i \sin(\beta_k) + v_j \sin(\alpha_k)] - \dot{\alpha}_k^* \\ &\quad + \lambda_3 \tilde{\alpha}_k + \nu_{\omega_k}, \quad (33b) \end{aligned}$$

where $\hat{\psi}_k$ is equivalent to (17) replacing ω_i by $\hat{\omega}_i$. We have the following.

Proposition 2: Consider $N - 1$ pairs of autonomous vehicles in a leader-follower configuration, each modelled as in (3) and forming a directed spanning tree —cf. Figure 2. Assume that the leader velocities are bounded, that is,

$$|v_i| < a_1, \quad |\dot{v}_i| < a_2, \quad |\omega_i| < a_3, \quad |\dot{\omega}_i| < a_4, \quad (34)$$

for all $i \in \{0, 1, \dots, N\}$. Then, for each vehicle, labeled j with $j \in \mathbb{N}_{\leq N}$, consider the controller defined by Eqs. (33a), (33b) with the observer (32a) (32b) for each $k \leq N - 1$. Then, the closed-loop trajectories corresponding to the formation errors $\tilde{\rho}_k$, $\tilde{\beta}_k$ and the velocity estimation errors \bar{v}_i , $\bar{\omega}_i$ are uniformly ultimately bounded. ■

Proof: Let $e_{2k} = [\tilde{\rho}_k \ \tilde{\beta}_k \ \tilde{\alpha}_k \ \bar{v}_i \ \bar{\omega}_i]^\top$ and consider the barrier Lyapunov function $V_{2k} : \mathcal{D}_k \times \mathbb{R}^4 \rightarrow \mathbb{R}_{\geq 0}$ defined as

$$V_{2k}(e_{2k}) := \frac{K_1}{2} \bar{v}_i^2 + \frac{K_1}{2} \bar{\omega}_i^2 + V_{1k}(\tilde{\rho}_k, \tilde{\beta}_k, \tilde{\alpha}_k), \quad (35)$$

which is positive definite and radially unbounded in its domain of definition. The total derivative of V_{2k} along the trajectories of the closed-loop dynamics yields

$$\dot{V}_{2k}(e_{2k}) = -\lambda_1 \left[\tilde{\rho}_k + \frac{\tilde{\rho}_k}{[\rho_k^{*2} - \tilde{\rho}_k^2]^{1/2}} \right]^2 - \lambda_2 \tilde{\beta}_k^2 \quad (36)$$

$$\begin{aligned} & -\lambda_3 \tilde{\alpha}_k^2 - \lambda_4 K_1 \bar{v}_i^2 - \lambda_5 K_2 \bar{\omega}_i^2 \\ & -K_2 \bar{v}_i [\lambda_4 v_i + \dot{v}_i] - K_2 \bar{\omega}_i [\lambda_5 \omega_i + \dot{\omega}_i]. \end{aligned}$$

Then, by simplifying the first term on the right-hand side of the previous inequality, we get

$$\begin{aligned} \dot{V}_{2k}(e_{2k}) \leq & -\lambda_1 \tilde{\rho}_k^2 - \lambda_2 \tilde{\beta}_k^2 - \lambda_3 \tilde{\alpha}_k^2 - \lambda_4 K_1 \bar{v}_i^2 \\ & -\lambda_5 K_2 \bar{\omega}_i^2 - K_1 \bar{v}_i [\lambda_4 v_i + \dot{v}_i] \\ & -K_2 \bar{\omega}_i [\lambda_5 \omega_i + \dot{\omega}_i]. \end{aligned} \quad (37)$$

Using (34), we obtain

$$\begin{aligned} \dot{V}_{2k}(e_{2k}) \leq & -\lambda_1 \tilde{\rho}_k^2 - \lambda_2 \tilde{\beta}_k^2 - \lambda_3 \tilde{\alpha}_k^2 - \lambda_4 K_1 \bar{v}_i^2 \\ & -\lambda_5 K_2 \bar{\omega}_i^2 + \lambda_4 K_1 |\bar{v}_i| \left[a_1 + \frac{a_2}{\lambda_4} \right] \\ & + \lambda_5 K_2 |\bar{\omega}_i| \left[a_3 + \frac{a_4}{\lambda_5} \right], \end{aligned} \quad (38)$$

which in turn implies

$$\begin{aligned} \dot{V}_{2k}(e_{2k}) \leq & -\lambda_1 \tilde{\rho}_k^2 - \lambda_2 \tilde{\beta}_k^2 - \lambda_3 \tilde{\alpha}_k^2 \\ & -\frac{\lambda_4 K_1}{2} \bar{v}_i^2 - \frac{\lambda_5 K_2}{2} \bar{\omega}_i^2 + b_i, \end{aligned} \quad (39)$$

where

$$b_i = \frac{\lambda_4 K_1}{2} \left[a_1 + \frac{a_2}{\lambda_4} \right]^2 + \frac{\lambda_5 K_2}{2} \left[a_3 + \frac{a_4}{\lambda_5} \right]^2. \quad (40)$$

Therefore, \dot{V}_{2k} is negative definite as long as,

$$\|e_{2k}\| > \epsilon := \sqrt{\frac{b_i}{\min\{\lambda_1, \lambda_2, \lambda_3, \frac{\lambda_4 K_1}{2}, \frac{\lambda_5 K_2}{2}\}}} \quad (41)$$

where ϵ represent the bounds of e_{2k} , the observer-closed-loop systems error. Finally, $\dot{V}_{2k}(e_{2k}) < 0$ holds outside a compact set and the GUUB of the solutions follows. ■

IV. SIMULATIONS

We carried out some numerical simulations using Simulink™ of Matlab™. The example consists in four uni-cycles following in diamond formation a fictitious leader vehicle—see Figure 3. The desired formation is defined by setting the desired orientations (in rad) β_k^* to $\beta_1^* = 0$, $\beta_2^* = \beta_4^* = \pi/6$, $\beta_3^* = -\pi/6$, and the desired distances to $\rho_k^* = 1$ m for all $k \in \{1, 2, 3, 4\}$.

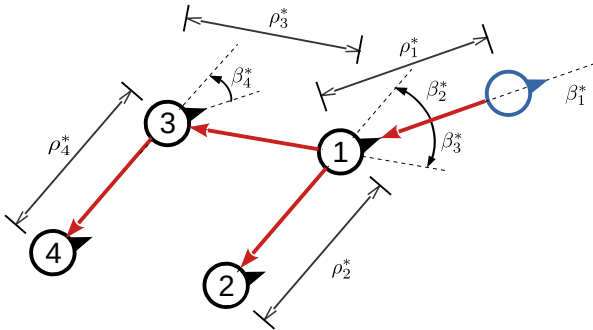


Fig. 3. Schematics of the desired physical formation of four robots following a fictitious leader vehicle (in blue) and the interconnections graph representation (links shown in red)

The controllers' gains are set to $\lambda_1 = \lambda_2 = \lambda_3 = 1$ and the observers' gains $\lambda_4 = \lambda_5 = 5$, $K_1 = K_2 = 20$. As initial conditions, we choose $\beta_1(0) = -0.2$ rad, $\beta_2(0) = \beta_3(0) = \beta_4(0) = 1$ rad, for the angle β_k . Moreover, the inter-vehicular distances are chosen $\rho_1(0) = 1.5$ m, $\rho_2(0) = 1.7$ m, $\rho_3(0) = 1.8$ m, $\rho_4(0) = 1.9$ m.

In Figures 4 we show the relative distances ρ_k converging to their respective references ρ_k^* ; in Figure 5 are depicted the desired relative orientations β_k also convergent to the desired values. The paths followed by the robots are shown in Figure 6.

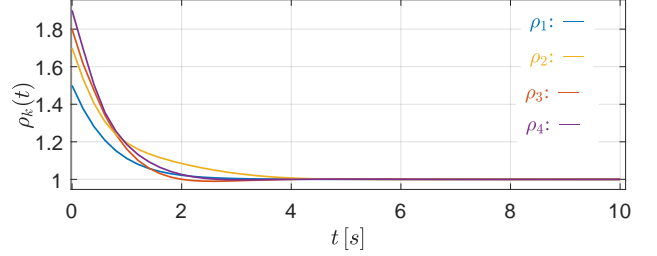


Fig. 4. Behavior of ρ_k

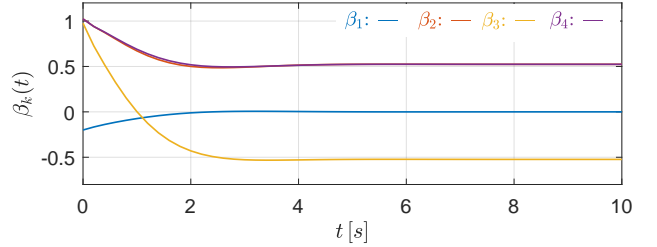


Fig. 5. Behavior of β_k

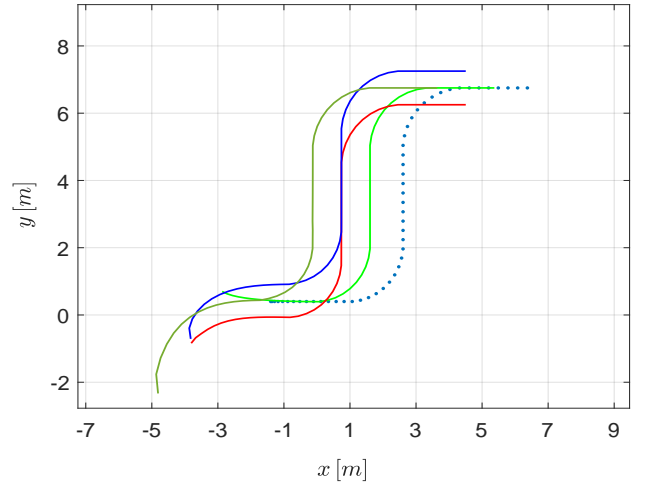


Fig. 6. Trajectories of the agents on the (x, y) -plane

In a second test we assume the leader's velocities to be unknown and we use the observer (32a), (32b). We notice in Figures 7, 8 representing the variables \bar{v}_i , $\bar{\omega}_i$ that these last ones converge towards a neighborhood of the origin, in other words, we see that these errors are bounded. Figure 9 presents the trajectories of the agents.

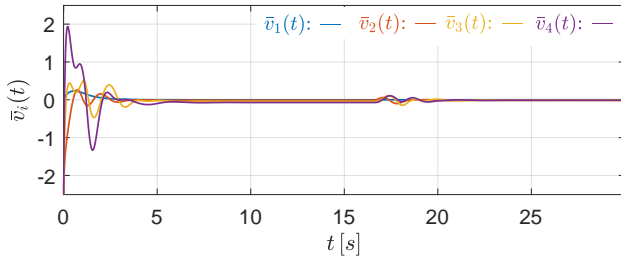


Fig. 7. Evolution of convergence errors $\bar{v}_i(t)$

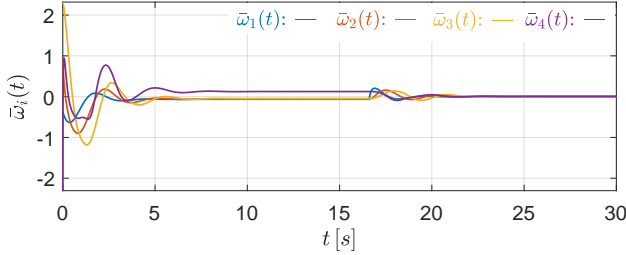


Fig. 8. Evolution of convergence errors $\bar{\omega}_i(t)$

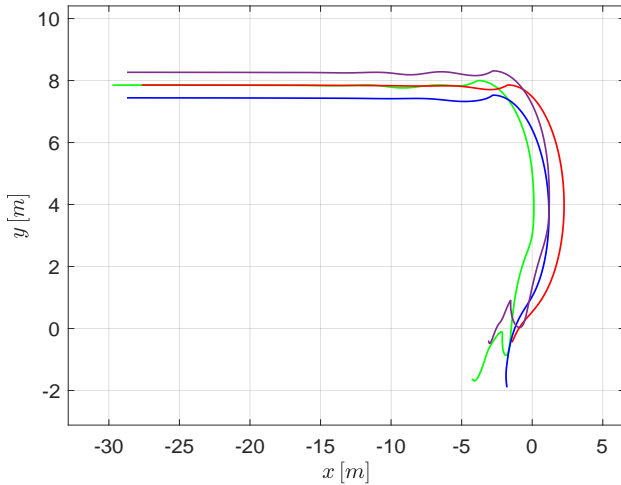


Fig. 9. Trajectories of the agents with velocities observer on the (x, y) -plane

V. CONCLUSION

The proposed control law ensures that a desired formation is achieved while simultaneously tracking a desired trajectory for a group of unicycles interconnected in a leader-follower configuration. For this purpose, we used a polar-coordinates model because of the advantages it offers, namely the ability to achieve the objective via smooth time-invariant feedback.

The control methodology is based on barrier Lyapunov functions and a polar-coordinates-based model that allowed us to transform the consensus-based formation problem into a stabilization problem that is more suited to be studied using Lyapunov theory. Then we used a certainty-equivalence controller to allow each agent to estimate the linear and angular velocity of its leader, which brings the proposed solution closer to reality. Current research is aimed at improving the performance by considering additional requirements for collision avoidance. In addition, further work is carried out

to enforce convergence of the estimation errors.

REFERENCES

- [1] Q. Yang, H. Fang, M. Cao, C. Shang, and Y. Wei, "Tunable formation realization for nonholonomic mobile robots using the stress matrix," in *2019 Chinese Control Conference (CCC)*, pp. 5853–5858, 2019.
- [2] Z. Wang, L. Wang, H. Zhang, and Q. Chen, "A graph based formation control of nonholonomic wheeled robots using a novel edge-weight function," in *2017 IEEE International Conference on Systems, Man, and Cybernetics (SMC)*, pp. 1477–1481, 2017.
- [3] Y. Wang, Z. Miao, H. Zhong, and Q. Pan, "Simultaneous stabilization and tracking of nonholonomic mobile robots: A Lyapunov-based approach," *IEEE Transactions on Control Systems Technology*, vol. 23, no. 4, pp. 1440–1450, 2015.
- [4] M. A. Maghenem, A. Loría, and E. Panteley, "Lyapunov-based formation-tracking control of nonholonomic systems under persistency of excitation," *IFAC-PapersOnLine*, vol. 49, pp. 404–409, 2016.
- [5] W. Fan and G. Zhiyong, "An approach to formation maneuvers of multiple nonholonomic agents using passivity techniques," in *2009 Chinese Control and Decision Conference*, pp. 5007–5012, 2009.
- [6] M. Maghenem, A. Loría, and E. Panteley, "Cascades-based leader-follower formation-tracking and stabilization of multiple nonholonomic vehicles," *IEEE Transactions on Automatic Control*, vol. 65, no. 8, pp. 3639–3646, 2019.
- [7] X. Li, M. J. Er, and J. Wang, "Time-varying formation control of nonholonomic multi-agent systems," in *2019 2nd International Conference on Intelligent Autonomous Systems (ICoIAS)*, pp. 118–123, 2019.
- [8] Q. Wang, H. Wang, S. Li, and Y. Zhang, "Bearing-only nonlinear formation control for nonholonomic unicycles," 2020.
- [9] M. Aicardi, G. Casalino, A. Bicchi, and A. Balestrino, "Closed loop steering of unicycle like vehicles via Lyapunov techniques," *IEEE Robotics and Automation Magazine*, vol. 2, pp. 27–35, Mar. 1995.
- [10] D. Shen, Z. Sun, and Y. Qiao, "Second-order sliding mode control for nonholonomic mobile robots formation," in *Proceedings of the 30th Chinese Control Conference*, pp. 4860–4864, 2011.
- [11] S.-L. Dai, S. He, X. Chen, and X. Jin, "Adaptive leader-follower formation control of nonholonomic mobile robots with prescribed transient and steady-state performance," *IEEE Transactions on Industrial Informatics*, vol. 16, no. 6, pp. 3662–3671, 2020.
- [12] B. Wang, S. Nersesov, and H. Ashrafiuon, "Formation regulation and tracking control for nonholonomic mobile robot networks using polar coordinates," *IEEE Control Systems Letters*, vol. 6, pp. 1909–1914, 2022.
- [13] Z. Miao, Y.-H. Liu, Y. Wang, G. Yi, and R. Fierro, "Distributed estimation and control for leader-following formations of nonholonomic mobile robots," *IEEE Transactions on Automation Science and Engineering*, vol. 15, no. 4, pp. 1946–1954, 2018.
- [14] X. Liang, H. Wang, Y.-H. Liu, Z. Liu, and W. Chen, "Leader-following formation control of nonholonomic mobile robots with velocity observers," *IEEE/ASME Transactions on Mechatronics*, vol. 25, no. 4, pp. 1747–1755, 2020.
- [15] H. Poonawala, A. C. Satici, N. Gans, and M. W. Spong, "Formation control of wheeled robots with vision-based position measurement," in *2012 American Control Conference (ACC)*, pp. 3173–3178, 2012.
- [16] E. Restrepo, I. Sarras, A. Loría, and J. Marzat, "Leader-follower consensus of unicycle-type vehicles via smooth time-invariant feedback," in *Proc. European Control Conference (ECC)*, pp. 917–922, 2020.
- [17] E. Restrepo, A. Loria, I. Sarras, and J. Marzat, "Robust consensus of high-order systems under output constraints: Application to rendezvous of underactuated UAVs," *IEEE Transactions on Automatic Control*, 2022.
- [18] J. Farrell, M. Polycarpou, M. Sharma, and W. Dong, "Command filtered backstepping," *IEEE Transaction on Automatic Control*, vol. 54, pp. 1391 – 1395, 07 2009.
- [19] I. Burkov, "Mechanical system stabilization via differential observers" in preprints of the IFAC Conf. on system structure and control. france, nantes: Ecole centrale de nantes, 1995. p. 532-535. postprint volume: Pergamon, p. 481-484., 01 1995.
- [20] A. Loría, "Observers are unnecessary for output-feedback control of Lagrangian systems," *IEEE Transactions on Automatic Control*, vol. 61, no. 4, pp. 905–920, 2016.